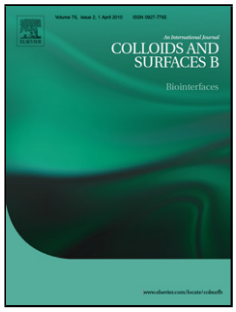

Hierarchy of Interactions Dictating the Thermodynamics of Real Cell Membranes: Following the Insulin Secretory Granules Paradigm up to Fifteen-Components Vesicles

Francesca Saitta (Conceptualization) (Methodology) (Investigation) (Validation) (Writing - review and editing), Marco Signorelli (Investigation)<ce:contributor-role>Data Curation), Dimitrios Fessas (Conceptualization) (Methodology) (Investigation) (Writing - review and editing) (Supervision) (Resources)

PII: S0927-7765(19)30859-8

DOI: https://doi.org/10.1016/j.colsurfb.2019.110715

Reference: COLSUB 110715

To appear in: *Colloids and Surfaces B: Biointerfaces*

Received Date: 5 August 2019

Revised Date: 9 November 2019

Accepted Date: 7 December 2019

Please cite this article as: Saitta F, Signorelli M, Fessas D, Hierarchy of Interactions Dictating the Thermodynamics of Real Cell Membranes: Following the Insulin Secretory Granules Paradigm up to Fifteen-Components Vesicles, *Colloids and Surfaces B: Biointerfaces* (2019), doi: https://doi.org/10.1016/j.colsurfb.2019.110715

Hierarchy of Interactions Dictating the Thermodynamics of Real Cell Membranes: Following the Insulin Secretory Granules Paradigm up to Fifteen-Components Vesicles

Francesca Saitta, Marco Signorelli and Dimitrios Fessas*

Dipartimento di Scienze per gli Alimenti, la Nutrizione e l'Ambiente, DeFENS, Università degli Studi di Milano, Via Celoria 2, 20133, Milano, Italy

*Corresponding author. E-mail address: dimitrios.fessas@unimi.it. Tel.: +39 0250319219

Graphical abstract

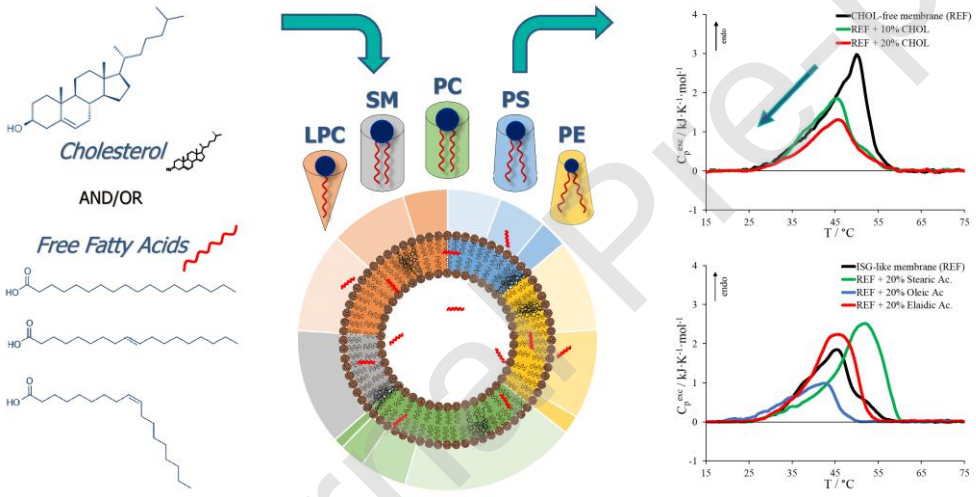

Highlights

- A phospholipid headgroup has minor effect than tail on mixed membranes cooperativity
- The preparation of a high-complexity fifteen-components membrane was achieved
- The type of thermodynamic effect of FFAs does not depend on membrane composition
- *Trans*-unsaturated FFAs have intermediate effects respect to *cis*- and saturated ones

1. Abstract:

A fifteen-components model membrane that reflected the 80% of phospholipids present in Insulin Secretory Granules was obtained and thermodynamic exploitation was performed, through micro-DSC, in order to assess the synergic contributions to the stability of a mixed complex system very close to real membranes. Simpler systems were also stepwise investigated, to complete a previous preliminary study and to highlight a hierarchy of interactions that can be now summarized as phospholipid tail unsaturation > phospholipid tail length > phospholipid headgroup > membrane curvature. In particular, Small Unilamellar Vesicles (SUVs) that consisted in phospholipids with different headgroups (choline, ethanolamine and serine), was step by step considered, following inclusion of sphingomyelins and lysophosphatidylcholines together with a more complete fatty acids distribution characterizing the phospholipid bilayer of the Insulin Secretory Granules. The inclusion of cholesterol was finally considered and the influence of three FFAs (stearic, oleic and elaidic acids) was investigated in comparison with simpler systems, highlighting the magnitude of the effects on such a detailed membrane in the frame of Type 2 Diabetes Mellitus alterations.

Keywords: Model membranes, Differential Scanning Calorimetry, Free Fatty Acids, Insulin Secretory Granules, Type 2 Diabetes Mellitus.

2. Introduction

The Insulin Secretory Granule (ISG) is a complex intracellular organelle of the pancreatic β-cell dedicated to insulin storage and secretion [1]. These subcellular vesicles have been characterized as phospholipid bilayer spheres of about 300nm of diameter [2,3] containing a crystalline core of insulin and zinc surrounded by a halo region of amylin (also known as Islet Amyloid Polypeptide, IAPP) together with other additional molecules [4,5]. However, such a granule is far more than just a repository of the hormones in the cell since it is the site of insulin proteolytic activation and it is involved in intercellular communication. Moreover, its membrane contains a variety of proteins which are key components for secretion control, different catalytic activities and messenger functions [3].

However, cells and vesicles functionalities are not only dependent on protein-based mechanisms. Indeed, lipid composition of phospholipid membranes severely affect their thermodynamic stability, which in turn is able to influence membrane proteins' functionality [6–8]. Moreover, among other external factors, the presence of Free Fatty Acids (FFAs) may severely affect the membrane thermotropic behaviour [9]. Low levels of FFAs are naturally present in biological membranes (around 0.3-10% of total lipids) [10] as well as in plasma. However, altered

FFAs levels are recurrent in diabetic and/or obese subjects and plasma FFAs concentration is generally high in both with levels that tend to be increasingly higher with weight gain [11].

Despite the numerous studies on model membranes carried out also including calorimetric techniques, such model systems were characterized by a simple composition which does not consider the complexity and the asymmetry of the real bilayers [12] and the lipid thermodynamic reorganization [13,14] that might be a key point for the correct interpretation of membrane-based mechanisms in cells since each lipid modification might produce a reorganization of the lipid molecules within such systems, which in turn might lead to variations of their physicochemical properties such as thermodynamic stability, permeability, fluidity, etc. [9,15].

In this frame, we started a stepwise study on the influence of the several parameters that may influence the IGS membrane thermodynamics. Indeed, in our previous work [9], we started from simple binary systems up to the preparation of a final model membranes whose phospholipids proportionally follow their abundancy and represent the 75% of the phospholipids' tails and the 50% of the headgroups in real ISGs [16]. In particular, we dissect the effects of morphology (membrane curvature), lipid composition focusing on the acyl chains keeping the same headgroup (phosphocholines with different acyl chains length and also in presence of unsaturations) and the free fatty acids (FFAs) action. In synthesis, we evidenced that curvature effects are mainly relevant among one-component unilamellar vesicles, whereas become of minor importance increasing the vesicle complexity. Moreover, the saturated phospholipids' contribution to the overall membrane stability is somehow "additive", whereas the presence of unsaturated phospholipids, even in minor amounts, has a relevant overall destabilizing effect and enhance the homogeneousness on the phases distribution. The entropic effects were hierarchically summarized as phospholipid unsaturations > phospholipid tail length > membrane curvature. As for the influence of FFAs, saturated acids produce a mainly strong entropic and enthalpic stabilizing effects, whereas the unsaturated ones produce an overall destabilization of the membranes.

In this work, we continued this step-by-step dissection following the ISGs composition and gradually including the influence of the different phospholipid headgroups, 16:0 LysoPC, sphingomyelins (egg sphingomyelin was used in this case) and cholesterol. Namely, we performed a thermodynamic study of different Small Unilamellar Vesicles (SUVs) at physiological pH by using the micro-DSC technique. At the first, vesicles were prepared as mixed system of DPPC, DPPS and DPPE in order to study how phospholipid headgroups affect the membrane thermodynamics. Then, 16:0 LysoPC and egg sphingomyelin were added reproducing the 80% of the headgroups and an average of 35% of the tails in real ISGs [16]. In order to integrate the acyl chain distribution, vesicles were therefore obtained by mixing fourteen different lipids, achieving a

composition which represents the 80% of the headgroups and an average of 80% of the tails in real ISGs. The inclusion of cholesterol was finally considered for the achievement of final ISG-like membrane. The influence of three FFAs (stearic, oleic and elaidic acids) was eventually investigated, in comparison with the previous study, highlighting the magnitude of the effects on such a detailed membrane.

3. Materials and methods

3.1. Materials

1,2-distearoyl-sn-glycero-3-phosphocholine (DSPC), 1,2-dipalmitoyl-sn-glycero-3-phosphocholine (DPPC), 1,2-dimyristoyl-sn-glycero-3-phosphocholine (DMPC), 1,2-dioleoyl-sn-glycero-3-phosphocholine (DOPC), 1,2-distearoyl-sn-glycero-3-phosphoethanolamine (DSPE), 1,2-dipalmitoyl-sn-glycero-3-phosphoethanolamine (DPPE), 1,2-dioleoyl-sn-glycero-3-phosphoethanolamine (DOPE), 1,2-distearoyl-sn-glycero-3-phospho-L-serine (DSPS, sodium salt), 1,2-dipalmitoyl-sn-glycero-3-phospho-L-serine (DPPS, sodium salt), 1,2-dioleoyl-sn-glycero-3-phospho-L-serine (DOPS, sodium salt), 1-palmitoyl-2-hydroxy-sn-glycero-3-phosphocholine (16:0 LPC), 1-behenoyl-2-hydroxy-sn-glycero-3-phosphocholine (22:0 LPC), 1-oleoyl-2-hydroxy-sn-glycero-3-phosphocholine (18:1 LPC), egg sphingomyelin (EggSM, Chicken) and cholesterol powders were purchased from Avanti Polar Lipids (purity certified by the supplier >99%), whereas stearic acid (SA), oleic acid (OA) and elaidic acid (EA) as well as the other chemicals, were obtained from Sigma-Aldrich. The lipids were of the highest available purity (≥99%) and were used without further purification. All solvents were of analytical grade.

3.2. Selection of vesicles constituents

The components mentioned above reflect the ISGs' fatty acid distribution [16] with the exception of EggSM that was preferred for practical reasons instead of the combination of synthetic sphingomyelins. EggSM was selected among other natural sphingomyelins, such as BrainSM and MilkSM, because of a higher similarity of the fatty acid distribution to those reported for the ISGs, according to the supplier's information (Egg SM – Avanti Number 860061 – Fatty Acids Distribution: 86% of 16:0, 6% of 18:0, 3% of 22:0, 3% of 24:1, 2% of unknown fraction).

3.3. Liposomes preparation

Liposomes were prepared through thin-film hydration [17]. An amount of about 20mg lipids were dissolved in chloroform:methanol 3:1 in a round-bottomed flask (mixtures that did not contain

the serine headgroup were dissolved in chloroform). Lipids were dried under a stream of dry nitrogen gas and evaporated to dryness through rotary evaporation (Heidolph Laborota 4000 efficient, WB eco, Schwabach, Germany) at 45°C. The films were kept under vacuum for at least 3 hours to remove solvent traces and then aged overnight at 4°C. For the hydration, 10mM phosphate buffer (pH 7.4) at a temperature above the gel-to-liquid crystalline transition of the lipid system was added up to a 10mg/mL lipid concentration. After the complete dispersion of the lipid films, the obtained mixtures were slowly stirred in water bath, at the same temperature chosen for the buffer, for about an hour until the induction of a homogenous suspension. The Multilamellar Lipid Vesicles MLVs dispersions obtained were extruded through polycarbonate filters (pore size of 100nm) mounted on a heated mini-extruder (Avanti Polar Lipids, Alabaster, AL, USA) fitted with two 1mL gastight syringes (Hamilton, Reno, NV, USA) in order to obtain suspensions of Small Unilamellar Vesicles (SUVs). An odd number of passages, usually 41, was performed to avoid any contamination by liposomes that might have not passed through the filters, as suggested elsewhere [18].

As for FFAs-containing membranes, the acids were mixed with phospholipids prior to dissolve them in chloroform:methanol 3:1.

According to our previous study [9], DLS data indicated that the described procedure produces SUVs with a size distribution around the nominal provided by the supplier (*i.e.* 100nm) and small deviations are not sufficient to influence the micro-DSC thermograms. For this reason, this characterization was not repeated here considering also that in the same study was observed that curvature effects are mainly visible for single-component systems, whereas they become negligible for multicomponent systems (broad DSC profiles) even in the presence of relevant differences in average size and size distributions [9].

3.4. Thermal analysis measurements

Calorimetry was used to determine the thermodynamic stability of the membranes with specific reference to the gel-to-liquid crystalline phase transitions.

Micro-DSC was selected as the most suitable technique for liposome investigation since low lipid concentrations are allowed to avoid vesicles – vesicles mutual interaction [19]. The instrument used was a Setaram micro DSCIII (Setaram Instrumentation, Caluire, France) operating with 1mL hermetically closed pans at 0.5°C/min scanning rate. After the conclusion of the liposomes' preparation protocols, each dispersion was allowed to anneal for at least 30 min at room temperature before launching the DSC measurement. SUVs samples were diluted up to 2.5mM

phospholipid concentration, also for vesicles which included FFAs. The final phospholipid concentration for all kind of vesicles was checked by the Stewart assay [20].

The raw data were worked out with the dedicated software "THESEUS" [21]. Briefly, the apparent specific heat trace, $C_p^{app}(T)$, was scaled to obtain the excess specific heat, $C_p^{exc}(T)$, with respect to the low temperature lipids state. Due to such a treatment, the area beneath the recorded peaks directly corresponded to the relevant transition enthalpy $\Delta H°$ of the lipid phase. Two or more heating-cooling cycles were applied to the samples to ensure reversibility and to exclude the presence of metastable phases. Up to the ternary membrane two cycles were enough, whilst for more complex systems more cycles were necessary to achieve reproducibility (see Supplementary Materials). In all cases, the last cycle thermograms were considered for analysis of the thermotropic transitions shown in figures. Errors were evaluated on the basis of at least three replicas.

In order to quantitatively compare and discuss the transition cooperativity between different systems, we adopted the transition average temperature, $\bar{T}$, and the average cooperativity index, *ACI*, defined elsewhere [9]. Briefly, the transition average temperature, $\bar{T}$, is defined as

$$\bar{T} = \int_{T_0}^{T_f} T \cdot f(T) dT$$

being T_0 and T_f the initial and final limit of the observable peak, respectively, and the frequency function $f(T)$ is the normalized calorimetric peak distribution

$$f(T) = \frac{C_p{}^{exc}(T)}{\Delta H°},$$

whereas the average cooperativity index, *ACI*, is defined as

$$ACI = \sqrt{\int_{T_0}^{T_f} (T - \bar{T})^2 \cdot f(T) dT}$$

Moreover, the $|\bar{T} - T_{max}|$ difference represents a peak asymmetry index.

4. Results and discussion

4.1. Phospholipid headgroups effects

In order to preliminary assess the mixing behaviour of systems with different phospholipid headgroup, we chose to use systems with same tail length (16:0). The micro-DSC thermograms of

SUVs with binary composition prepared at 1:1 molar ratio of DPPC:DPPE, DPPC:DPPS and DPPS:DPPE are reported in Fig.1a.

Fig1.approximately.here

We observed broad profiles typical of unilamellar vesicles with mixed composition, *i.e.* less cooperative respect to the single-component vesicles [9], corresponding to the main gel-to-liquid crystalline phase transition. In each case the transition range was located between the transition T_{max} of the respective single-component dispersions [9,22–25] (also indicated in the figure by the vertical dotted lines). In first approximation, the absence of evident shoulders and the position of such profiles indicate that phospholipids with different headgroups, such as choline, ethanolamine and serine are thermodynamically compatible, *i.e.* miscible, despite the difference in phospholipid headgroups' size and charge. In order to better quantify these effects, the breadth of the peaks was described through the *Average Cooperativity Index* (*ACI*) (Table 1). In Fig.1b, the correlation of ACI values with the gap between the T_{max} values of the respective single-component systems, $\Delta_{s\text{-}c}T_{max}$, is highlighted. For the sake of comparison, the correlation obtained for the ACI values of the systems described in our previous work [9] regarding binary phospholipid systems with same headgroup (choline) and different acyl chains (myristoyl, palmitoyl and stearoyl chains) is also reported in the same figure. We observed that the loss of cooperativity well follows the $\Delta_{s\text{-}c}T_{max}$ gap in both cases, *i.e.* systems composed by saturated phospholipids. However, the loss of cooperativity due to differences in headgroups is less pronounced than that produced by differences in tails length, which in turn are able to produce a more severe dispersion of the membrane's thermodynamic phases.

The overall enthalpies, the peak maximum temperature values, T_{max}, and the transition average temperature, $\bar{T}$, obtained for the three binary mixtures here investigated are collected in Table 1. Indeed, for such dispersed and asymmetric profiles the $\bar{T}$ is more representative than the T_{max} since the overall phase distribution is considered. The $|\bar{T} - T_{max}|$ value obtained by data reported in Table 1 was 1.1°C for DPPC:DPPS, 2.5°C for DPPC:DPPE, 0.8°C for DPPS:DPPE and can be considered as an asymmetry index.

We observed that the $\bar{T}$ values were very close to the expected temperatures, $T_{expected}$, obtained by simply combining the T_{max} of the respective single-component systems. Furthermore, the overall enthalpies observed resulted to be additive to those observed for the single-components. This highlighted that there is not any relevant extra enthalpic contribution due to interaction between different headgroups, hence revealing that the thermotropic behaviour of these vesicles is mainly

entropically driven. Similar additivity effects and entropically driven phenomena were also observed for differences in tail lenghts [9].

Fig2.approximately.here

In order to confirm the proportionality of these effects highlighted in 1:1 saturated phospholipids binary systems, a model membrane with a ternary composition was obtained by combining the same phospholipid used so far and reflecting the proportions observed in the ISGs (4.5 DPPC : 3.5 DPPE : 2 DPPS). Its calorimetric profile is represented by the curve in Fig.2a. We observed an asymmetric peak for which the $\bar{T}$ value (52.4 ± 0.1°C) was comparable to the $T_{expected}$ (52.3°C) obtained from the constituents' T_{max}. Moreover, the overall enthalpy resulted to be still additive, confirming the conclusions achieved for the 1:1 binary mixtures.

The overall picture in terms of correlation between the $\bar{T}$ and $T_{expected}$ (also integrating data from [9] concerning the tails length dependence, namely the DMPC:DPPC, DMPC:DSPC and DPPC:DSPC 1:1 binary systems) is represented by Fig.2b. We observed an almost linear correlation between the observed $\bar{T}$ and the $T_{expected}$. According to these results, we may argue that the trends of $\bar{T}$ and enthalpic stability proportionally follow the constituents' contributions in case of phospholipids with saturated acyl chains, indicating high thermodynamic compatibility of such species. Furthermore, the strong proportionality shown in Fig.2b highlights that predictions on the position of the calorimetric profiles, in terms of $\bar{T}$, are allowed and deviations from linearity in the $\bar{T}$ vs $T_{expected}$ plane might be used to detect other type of interactions due to different vesicle constituents than the saturated phospholipids and/or to the presence of external agents (as FFAs in our case) that may affect the phospholipid packing (see Supplementary Material).

As regards the hierarchy of interactions, the thermodynamic information here obtained allowed us to complete the previously delineated one [9], including the effect of headgroup differences. The overall information indicated that the strength of the effects can be catalogued as

membrane curvature < <u>phospholipid headgroup</u> < phospholipid tail length < phospholipid tail unsaturation.

In particular: membrane curvature effects become negligible for multi-components systems prepared as SUVs and/or as vesicles with a bigger size; headgroups and tails length produce effects for which the enthalpy and the $\bar{T}$ proportionally follow the single-components contributions and the loss of overall cooperativity depends on the transition temperature gap between the constituents

(this last effect is less pronounced for headgroups than tails length differences); the presence of phospholipid tail unsaturation is the factor that produces the most severe effect on membrane thermotropic behaviour by generally destabilizing it both in terms of enthalpy, transition temperature and cooperativity. In principle, by knowing such hierarchy of interaction, simpler *ad hoc* model membranes that reflect the behaviour of more complex ones might be prepared.

Following this stepwise investigation, a model membrane that reflected the major macro-categories constituting the ISGs [16] (phosphatidylcholines, phosphatidylethanolamines, phosphatidylserines, sphingomyelins and lysophosphatidylcholines) was considered, namely 2.80 DPPC : 2.15 DPPE : 1.40 DPPS : 2.40 16:0LPC : 1.25 EggSM (Fig.3a). The composition of such a preparation reflects the 80% of the headgroups and an average of 35% of the tails in real ISGs. The new components slightly differ from the previous ones investigated in the ternary membrane in terms of molecular geometry and chemical structure. Indeed, lysophosphatidylcholine has a peculiar conical shape because of the loss of one of the two acyl chains existing in a phospholipid, which instead has a cylindrical shape, whereas an acyl chain and the glycerol of phospholipids are replaced by a sphingosine molecule in sphingomyelin. As for the last component, EggSM was used, whose fatty acids distribution mainly consists in 16:0 chains (86%) according to the supplier's information.

The micro-DSC profile of the resulting five-components model membrane is reported in Fig.3b and the relative thermodynamic parameters are reported in Table 1. We observed an asymmetric and biphasic profile, index of phase separation. The introduction of the two new components in ISG's proportions produced a destabilizing entropic effect with loss of overall cooperativity (see ACI) and the transition range was shifted toward lower temperatures ($\bar{T}$ = 47.2 ± 0.3°C) with respect to the ternary membrane. On the other hand, a slight increase in overall transition enthalpy was observed. Considering that a phase separation was observed, we may argue that the high-stability lipid phases (detected in the high-temperature part the thermogram) might have been mostly interested by an enhancement of packing interactions, justifying the increase of transition enthalpy.

Despite sphingomyelin is reported in the literature to generate phase separation [26,27] and also some information is known on 16:0 LPC effects [28], specifically attributing the observed effects to one of these two components is beyond our scope, since an even more in-depth thermodynamic dissection of the contributions becomes more difficult when molecules that disturb the regular packing of the hydrophobic chains within the bilayer are present, *e.g.* unsaturated acyl chains [9], cholesterol [29,30], etc. Nonetheless, for clarity, the single contributions deriving by the addition of EggSM and 16:0 LPC separately to the headgroups ternary membrane was experimentally assessed

(see supplementary) confirming that both generate phase separations contributing to the final biphasic profile observed for the five-components membrane though the temperature range covered by the transition seems, qualitatively, more compatible with the EggSM addition.

This part of the stepwise evaluation was focused to the headgroups' thermodynamic contribution on the stability of phospholipid bilayers and was achieved by keeping the phospholipid tails length constant specular to the previous study which specifically devoted to tails effects by keeping the headgroups constant [9].

In order to integrate all the contributions considered and to conclusively simulate the ISGs lipid bilayers at our best, we achieved the preparation of a fourteen-components model membrane by proportionally selecting the most abundant acyl chains for each macro-category that inspired the five-component system. Details of this membrane composition are reported in Fig.3a. This system is very close to the phospholipid composition of the real ISG and achieves the 80% of representativeness in terms of both headgroups and acyl chains [16]. However, despite one of the most noteworthy components of most of the real cell membranes including ISGs is cholesterol, it was omitted in this preparation to allow a specific analysis of phospholipid interactions and will be taken into account in the next session in order to separately verify and discriminate its effects on the overall system.

Fig3.approximately.here

The micro-DSC profile of such fourteen-components membrane is reported in Fig.3b. We observed that the introduction of acyl chains differences severally enhanced the micro-DSC profile asymmetry and the loss of cooperativity compared to the one obtained for the five-components membrane (ACI values of 6.3 ± 0.2°C vs 3.8 ± 0.2°C for the five components). Moreover, the overall transition range was slightly extended toward both lower and higher temperatures, whereas the transition enthalpy significantly decreased. On the other hand, the phase separation previously seen for the five-components membrane seemed to be preserved. All these effects are coherent with the information's achieved so far, *i.e.* the higher composition complexity justifies the cooperativity loss, whereas the cooperativity and enthalpy loss are in line with the presence of about 11.7% of oleoyl chains since unsaturated acyl chains are known to destabilize the membrane stability from both an entropic and an enthalpic point of view [9]. The slight extension of the overall transition range to higher temperature than the five-components membrane may be ascribable to the presence of 23.3% of stearoyl chains.

4.2. ISG-like model membrane: influence of cholesterol

To conclude this stepwise investigation, we considered the action of cholesterol in membrane thermotropic behaviour, achieving the preparation of two fifteen-components membranes by the addition of cholesterol at different percentages (10% and 20%).

Fig4.approximately.here

The relative thermograms are shown in Fig.4 in comparison with the fourteen-components membrane. We observed a strong destabilizing effect with a progressive enthalpy depletion that depended on cholesterol amount, whereas the overall transition range remained almost the same. In particular, with the inclusion of 10% of cholesterol we observed a depletion of the signal in correspondence with the most stable phases, revealing a selective action of cholesterol to major affect the most ordered and/or stable regions [31]. However, the increase of the perturbing molecule concentration up to 20% also influenced the less stable lipid population.

In conclusion, cholesterol inclusion led to a membrane with big destabilized part. Roughly, if we assume an average enthalpic contribution, the ratio of the observed enthalpies indicated systems with about 30% and 50% of phospholipids in a disordered state for 10% and 20% cholesterol addition, respectively, and the phase distribution of the remaining part was spread in a large transition range (25 – 50 °C).

This scenario is very close to reality, *i.e.* compatible with the literature based on the fluid-mosaic model [32] and reflected the versatility of real membranes, which can explore both fluid and ordered regions in order to fulfil the necessity dictated by the several intermembrane proteins and cellular mechanisms.

4.3. ISG-like model membrane: influence of FFAs

Although the percentage of cholesterol within cell membranes may vary from very small amounts up to 50-60% in specific systems [33–35], as regard the action of external agents, namely FFAs in our case, we selected the fifteen-components membrane containing 10% cholesterol as reference final membrane to be indicated as reference ISG-like membrane in order to keep the micro-DSC signals well detectable.

Fig5.approximately.here

The effect of 20% addition stearic and oleic acids on cell membrane thermodynamics is reported in Fig.5a and the relevant thermodynamic parameters are reported in Table 1. At a first glance, Fig.5a shows stabilizing effects for the saturated FFA (stearic acid, dashed green curve) and destabilizing effects for the unsaturated FFA (oleic acid, dotted blue curve), revealing a similar scenario obtained in our previous work for less complex membranes [9]. Such respective stabilization and destabilization were also observed in terms of enthalpic contribution (Table 1). Since these observations are in line with those obtained from the previous investigations, we may conclude that the type of effects of FFAs observed are almost of the same nature regardless of the membrane lipid composition. Main composition-dependent differences may only be revealed in terms of magnitude of stabilization or destabilization of the membrane thermodynamics.

To complete the pattern, we included in this study the influence of a *trans*-unsaturated FFA as the elaidic acid on the ISG-like membrane. The resulting micro-DSC profile is reported as dashed red trace in Fig.5b. We observed a different effect with respect to the corresponded *cis*-unsaturated FFA (oleic acid), *i.e.* a mainly enthalpic stabilization effect. This behaviour is also in line with our conclusions for which, if we consider that the presence of a *trans* double bond makes such FFA linear, we expect it to be packable within the vesicle hydrophobic core analogously to stearic acid. However, despite the common stabilization, the effect was minor as regards both the enthalpic and the entropic contributions, suggesting peculiarities in the incorporation of elaidic acid. Since we may not exclude contributions compensations, we only limit to describe the experimental evidence that represents the overall effect.

In this study, we investigated the intrinsic membrane thermodynamics being aware that the *in vivo* cell membranes the phospholipid composition and distribution across the inner and the outer leaflets are not only regulated by triggered protein-independent processes as thermodynamic rearrangements [13,14,36], but may also directly depend on proteins action [8,37–39].

However, the thermograms obtained in this study for our final cholesterol-free (*i.e.* the fourteen-components vesicles) and ISG-like membranes exhibited very similar type of profiles to the ones reported in literature for both real cholesterol-free and cholesterol-containing cell membrane [40,41]. Although these indications regard different systems and are qualitative, the typical multicomponent membrane profiles observed support the suggestion that the real membrane peculiarities do not compromise the general conclusions here presented about the membrane thermodynamics, the influence of cholesterol and the effects of FFAs.

5. Conclusions

In this paper we completed a stepwise thermodynamic study on the contributions of the phospholipid constituents in the cell membrane stability keeping the phospholipid bilayer of ISGs as reference system.

The results permitted to integrate the hierarchy of influence on membrane thermodynamic stability that may be resumed as: membrane curvature < phospholipid headgroup < phospholipid tail length < phospholipid tail unsaturation. Saturated phospholipids are thermodynamically compatible and their influence on the thermotropic behaviour of the membrane is somehow "additive", *i.e.* their contribution are proportional to the lipid composition. As for the other components, as unsaturated acyl chains, sphingomyelin, etc., the description of the influence is less simple since they are able to generate visible entropic and enthalpic destabilization but their effects do not follow the linear trend highlighted by the saturated phospholipids. However, it emerged that in multi-components systems all the effects are mediated, limiting the presence of severe phase separations.

The influence of cholesterol led to a strong membrane order loss. Specifically, the effect of cholesterol depended on the added amount, revealing a preferable action on the most stable phases, whereas the less stable phases where impaired at higher cholesterol percentages. As for the FFAs influence, we figured out that the stabilizing effects of saturated FFAs and the destabilizing effects of *cis*-unsaturated FFAs occurs regardless of the membrane lipid composition. On the other hand, *trans*-unsaturated FFAs produce modest stabilizing effects mainly of ethalpic nature.

Finally, despite a real cell membrane is much more complex because of other non-lipid constituents as proteins and/or environmental conditions, etc., literature data [40,41] suggest that these peculiarities seem to not compromise the general conclusions here presented about the membrane thermodynamics, the influence of cholesterol and the effects of FFAs.

Authors Contributions

Author: Francesca Saitta

Conceptualization, Methodology, Investigation, Validation, Writing - Review & Editing

Author: Marco Signorelli

Investigation, Data Curation

Corresponding Author: Dimitrios Fessas

Conceptualization, Methodology, Investigation, Writing - Review & Editing, Supervision, Resources

Declaration-of-competing-interests

The authors declare that they have no known competing financial interests or personal relationships that could have appeared to influence the work reported in this paper.

References

[1] A. Young, Tissue Expression and Secretion of Amylin, in: Adv. Pharmacol., 2005: pp. 19–45. doi:10.1016/S1054-3589(05)52002-7.

[2] C.S. Olofsson, S.O. Göpel, S. Barg, J. Galvanovskis, X. Ma, A. Salehi, P. Rorsman, L. Eliasson, Fast insulin secretion reflects exocytosis of docked granules in mouse pancreatic B-cells, Pflügers Arch - Eur J Physiol. 444 (2002) 43–51. doi:10.1007/s00424-002-0781-5.

[3] J.C. Hutton, The insulin secretory granule, Diabetologia. 32 (1989) 271–281. doi:10.1007/BF00265542.

[4] P. Westermark, Z.-C. Li, G.T. Westermark, A. Leckström, D.F. Steiner, Effects of beta cell granule components on human islet amyloid polypeptide fibril formation, FEBS Lett. 379 (1996) 203–206. doi:10.1016/0014-5793(95)01512-4.

[5] J.C. Hutton, E.J. Penn, M. Peshavaria, Isolation and characterisation of insulin secretory granules from a rat islet cell tumour, Diabetologia. 23 (1982) 365–373. doi:10.1007/BF00253746.

[6] W. Zhang, M. Bogdanov, J. Pi, A.J. Pittard, W. Dowhan, Reversible Topological Organization within a Polytopic Membrane Protein Is Governed by a Change in Membrane Phospholipid Composition, J. Biol. Chem. 278 (2003) 50128–50135. doi:10.1074/jbc.M309840200.

[7] O.H. Samuli Ollila, T. Róg, M. Karttunen, I. Vattulainen, Role of sterol type on lateral pressure profiles of lipid membranes affecting membrane protein functionality: Comparison between cholesterol, desmosterol, 7-dehydrocholesterol and ketosterol, J. Struct. Biol. 159 (2007) 311–323. doi:10.1016/j.jsb.2007.01.012.

[8] T. Heimburg, B. Angerstein, D. Marsh, Binding of Peripheral Proteins to Mixed Lipid Membranes: Effect of Lipid Demixing upon Binding, Biophys. J. 76 (1999) 2575–2586. doi:10.1016/S0006-3495(99)77410-2.

[9] F. Saitta, M. Signorelli, D. Fessas, Dissecting the effects of free fatty acids on the thermodynamic stability of complex model membranes mimicking insulin secretory granules, Colloids Surfaces B Biointerfaces. 176 (2019) 167–175. doi:10.1016/j.colsurfb.2018.12.066.

[10] L.J. O'Connor, T. Nicholas, R.M. Levin, Subcellular Distribution of Free Fatty Acids, Phospholipids, and Endogenous Lipase Activity of Rabbit Urinary Bladder Smooth Muscle and Mucosa, in: Adv. Bl. Res., Springer, Boston, MA, 1999: pp. 265–273. doi:10.1007/978-1-4615-4737-2_20.

[11] P. Björntorp, H. Bergman, E. Varnauskas, Plasma free fatty acid turnover rate in obesity, Acta Med. Scand. 185 (1969) 351–356. doi:10.1111/j.0954-6820.1969.tb07347.x.

[12] J.E. Rothman, J. Lenard, Membrane Asymmetry, Science (80-.). 195 (1977) 743–753.

[13] P.L. Yeagle, J.E. Young, Factors contributing to the distribution of cholesterol among phospholipid vesicles, J. Biol. Chem. 261 (1986) 8175–8181. http://www.jbc.org/content/261/18/8175.short.

[14] K. Boesze-Battaglia, R. Schimmel, Cell membrane lipid composition and distribution: implications for cell function and lessons learned from photoreceptors and platelets., J. Exp. Biol. 200 (1997) 2927–2936. http://www.ncbi.nlm.nih.gov/pubmed/9359876.

[15] P. Losada-Pérez, N. Mertens, B. de Medio-Vasconcelos, E. Slenders, J. Leys, M. Peeters, B. van Grinsven, J. Gruber, C. Glorieux, H. Pfeiffer, P. Wagner, J. Thoen, Phase Transitions of Binary Lipid Mixtures: A Combined Study by Adiabatic Scanning Calorimetry and Quartz Crystal Microbalance with Dissipation Monitoring, Adv. Condens. Matter Phys. 2015 (2015) 1–14. doi:10.1155/2015/479318.

[16] M.J. MacDonald, L. Ade, J.M. Ntambi, I.-U.H. Ansari, S.W. Stoker, Characterization of Phospholipids in Insulin Secretory Granules and Mitochondria in Pancreatic Beta Cells and Their Changes with Glucose Stimulation, J. Biol. Chem. 290 (2015) 11075–11092. doi:10.1074/jbc.M114.628420.

[17] A. Laouini, C. Jaafar-Maalej, I. Limayem-Blouza, S. Sfar, C. Charcosset, H. Fessi, Preparation, Characterization and Applications of Liposomes: State of the Art, J. Colloid Sci. Biotechnol. 1 (2012) 147–168. doi:10.1166/jcsb.2012.1020.

[18] R.C. MacDonald, R.I. MacDonald, B.P.M. Menco, K. Takeshita, N.K. Subbarao, L. Hu, Small-volume extrusion apparatus for preparation of large, unilamellar vesicles, Biochim. Biophys. Acta - Biomembr. 1061 (1991) 297–303. doi:10.1016/0005-2736(91)90295-J.

[19] K. Gardikis, S. Hatziantoniou, M. Signorelli, M. Pusceddu, M. Micha-Screttas, A. Schiraldi, C. Demetzos, D. Fessas, Thermodynamic and structural characterization of Liposomal-Locked in-Dendrimers as drug carriers, Colloids Surfaces B Biointerfaces. 81 (2010) 11–19. doi:10.1016/j.colsurfb.2010.06.010.

[20] J.C.M. Stewart, Colorimetric determination of phospholipids with ammonium ferrothiocyanate, Anal. Biochem. 104 (1980) 10–14. doi:10.1016/0003-2697(80)90269-9.

[21] G. Barone, P. Del Vecchio, D. Fessas, C. Giancola, G. Graziano, THESEUS: A new software package for the handling and analysis of thermal denaturation data of biological macromolecules, J. Therm. Anal. 38 (1992) 2779–2790. doi:10.1007/BF01979752.

[22] S. Mabrey, J.M. Sturtevant, Investigation of phase transitions of lipids and lipid mixtures by sensitivity differential scanning calorimetry., Proc. Natl. Acad. Sci. 73 (1976) 3862–3866. doi:10.1073/pnas.73.11.3862.

[23] T.P.W. McMullen, R.N.A.H. Lewis, R.N. McElhaney, Calorimetric and spectroscopic studies of the effects of cholesterol on the thermotropic phase behavior and organization of a homologous series of linear saturated phosphatidylethanolamine bilayers, Biochim. Biophys. Acta - Biomembr. 1416 (1999) 119–134. doi:10.1016/S0005-2736(98)00214-4.

[24] C. Galvagnion, J.W.P. Brown, M.M. Ouberai, P. Flagmeier, M. Vendruscolo, A.K. Buell, E. Sparr, C.M. Dobson, Chemical properties of lipids strongly affect the kinetics of the membrane-induced aggregation of α-synuclein, Proc. Natl. Acad. Sci. 113 (2016) 7065–7070. doi:10.1073/pnas.1601899113.

[25] D. Bach, E. Wachtel, Thermotropic properties of mixtures of negatively charged phospholipids with cholesterol in the presence and absence of Li+ or Ca2+ ions, Biochim. Biophys. Acta - Biomembr. 979 (1989) 11–19. doi:10.1016/0005-2736(89)90517-8.

[26] T.-Y. Wang, J.R. Silvius, Sphingolipid Partitioning into Ordered Domains in Cholesterol-Free and Cholesterol-Containing Lipid Bilayers, Biophys. J. 84 (2003) 367–378. doi:10.1016/S0006-3495(03)74857-7.

[27] S.H. Untrach, G. Graham, Molecular interactions between lecithin and sphingomyelin. Temperature-and composition-dependent phase separation., J. Biol. Chem. 252 (1977) 4449–4457.

[28] C.J.A. Van Echteld, B. De Kruijff, J. De Gier, Differential miscibility properties of various phosphatidylcholine/lysophosphatidylcholine mixtures, Biochim. Biophys. Acta - Biomembr. 595 (1980) 71–81. doi:10.1016/0005-2736(80)90249-7.

[29] C. Wolf, K. Koumanov, B. Tenchov, P.J. Quinn, Cholesterol favors phase separation of sphingomyelin, Biophys. Chem. 89 (2001) 163–172. doi:10.1016/S0301-4622(00)00226-X.

[30] T. Shigematsu, K. Koshiyama, S. Wada, Molecular dynamics simulations of pore formation in stretched phospholipid/cholesterol bilayers, Chem. Phys. Lipids. 183 (2014) 43–49. doi:10.1016/j.chemphyslip.2014.05.005.

[31] T.P.W. McMullen, R.N. McElhaney, Differential Scanning Calorimetric Studies of the Interaction of Cholesterol with Distearoyl and Dielaidoyl Molecular Species of Phosphatidylcholine, Phosphatidylethanolamine, and Phosphatidylserine, Biochemistry. 36 (1997) 4979–4986. doi:10.1021/bi962815j.

[32] G.L. Nicolson, The Fluid—Mosaic Model of Membrane Structure: Still relevant to understanding the structure, function and dynamics of biological membranes after more than 40years, Biochim. Biophys. Acta - Biomembr. 1838 (2014) 1451–1466. doi:10.1016/j.bbamem.2013.10.019.

[33] M. Tsuchiya, M. Hosaka, T. Moriguchi, S. Zhang, M. Suda, H. Yokota-Hashimoto, K.

Shinozuka, T. Takeuchi, Cholesterol Biosynthesis Pathway Intermediates and Inhibitors Regulate Glucose-Stimulated Insulin Secretion and Secretory Granule Formation in Pancreatic β-Cells, Endocrinology. 151 (2010) 4705–4716. doi:10.1210/en.2010-0623.

[34] P.L. Yeagle, Cholesterol and the cell membrane, Biochim. Biophys. Acta - Rev. Biomembr. 822 (1985) 267–287.

[35] G. van Meer, A.I.P.M. de Kroon, Lipid map of the mammalian cell, J. Cell Sci. 124 (2011) 5–8. doi:10.1242/jcs.071233.

[36] H.J. Risselada, S.J. Marrink, Curvature effects on lipid packing and dynamics in liposomes revealed by coarse grained molecular dynamics simulations, Phys. Chem. Chem. Phys. 11 (2009) 2056. doi:10.1039/b818782g.

[37] E. Sezgin, I. Levental, S. Mayor, C. Eggeling, The mystery of membrane organization: composition, regulation and roles of lipid rafts, Nat. Rev. Mol. Cell Biol. 18 (2017) 361–374. doi:10.1038/nrm.2017.16.

[38] D.L. Daleke, Regulation of transbilayer plasma membrane phospholipid asymmetry, J. Lipid Res. 44 (2003) 233–242. doi:10.1194/jlr.R200019-JLR200.

[39] W. Römer, L.-L. Pontani, B. Sorre, C. Rentero, L. Berland, V. Chambon, C. Lamaze, P. Bassereau, C. Sykes, K. Gaus, L. Johannes, Actin Dynamics Drive Membrane Reorganization and Scission in Clathrin-Independent Endocytosis, Cell. 140 (2010) 540–553. doi:10.1016/j.cell.2010.01.010.

[40] B. de Kruyff, R.A. Demel, L.L.M. dan Deenen, The effect of cholesterol and epicholesterol incorporation on the permeability and on the phase transition of intact Acholeplasma laidlawii cell membranes and derived liposomes, Biochim. Biophys. Acta - Biomembr. 255 (1972) 331–347. doi:10.1016/0005-2736(72)90032-6.

[41] B.M. Mackey, C.A. Miles, S.E. Parsons, D.A. Seymour, Thermal denaturation of whole cells and cell components of Escherichia coli examined by differential scanning calorimetry, J. Gen. Microbiol. 137 (1991) 2361–2374. doi:10.1099/00221287-137-10-2361.

Figure captions

Fig.1

a) Micro-DSC thermograms for vesicles obtained by 1:1 DPPC:DPPE, DPPC:DPPS and DPPS:DPPE mixtures. The dotted vertical lines mark the T_{max} of pure DPPC, DPPS and DPPE MLBs (Multilamellar Lipid Bilayers, left to right). b) Graphical representation of the influence of the gap between the T_{max} values of the respective single-component systems, $\Delta_{s\text{-}c}T_{max}$, on thermograms breadth represented by ACI when generated by differences in headgroups or acyl chain length [9].

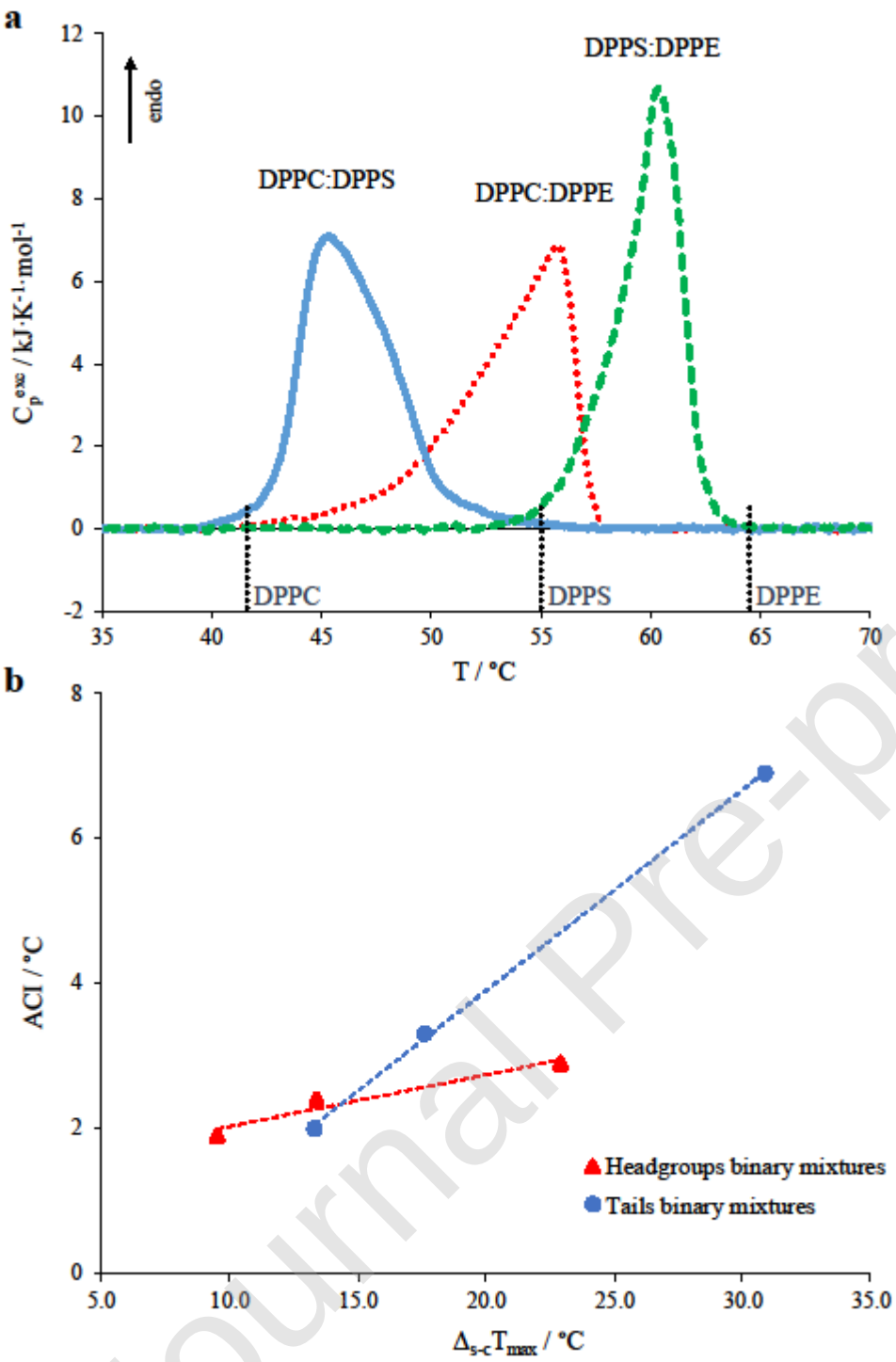

Fig.2

a) Micro-DSC thermogram for vesicles obtained as 4.5 DPPC : 3.5 DPPE : 2 DPPS. The dotted vertical lines mark the T_{max} of pure DPPC, DPPS and DPPE MLBs (Multilamellar Lipid Bilayers, left to right). b) Graphical representation of the transition average temperature, $\bar{T}$, of several representative model membranes versus the temperature expected by combining the T_{max} of the respective single-component systems, $T_{expected}$ (the "Tails" data where integrated from [9]).

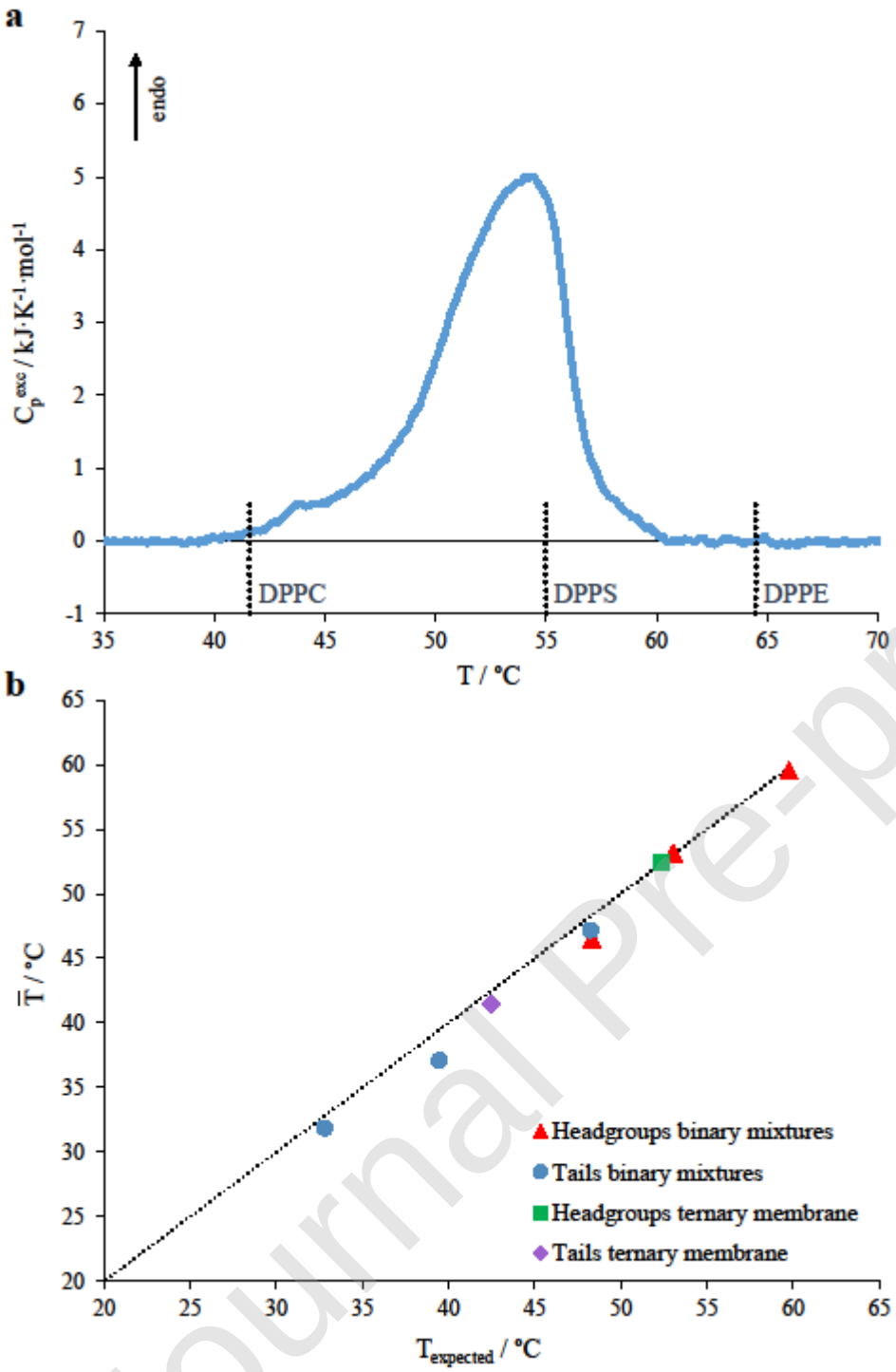

Fig.3

a) Diagrams representing, on the left, the composition of the five-components membrane (inner cycle) and the fourteen-components model membrane mimicking the ISG (outer cycle). The detailed percentages highlighting the acyl chains involved in the fourteen-components vesicles are reported on the right. b) Micro-DSC thermograms for the five-components model membrane (dotted red curve) and the fourteen-components membrane (solid black curve) prepared with compositions as in panel a.

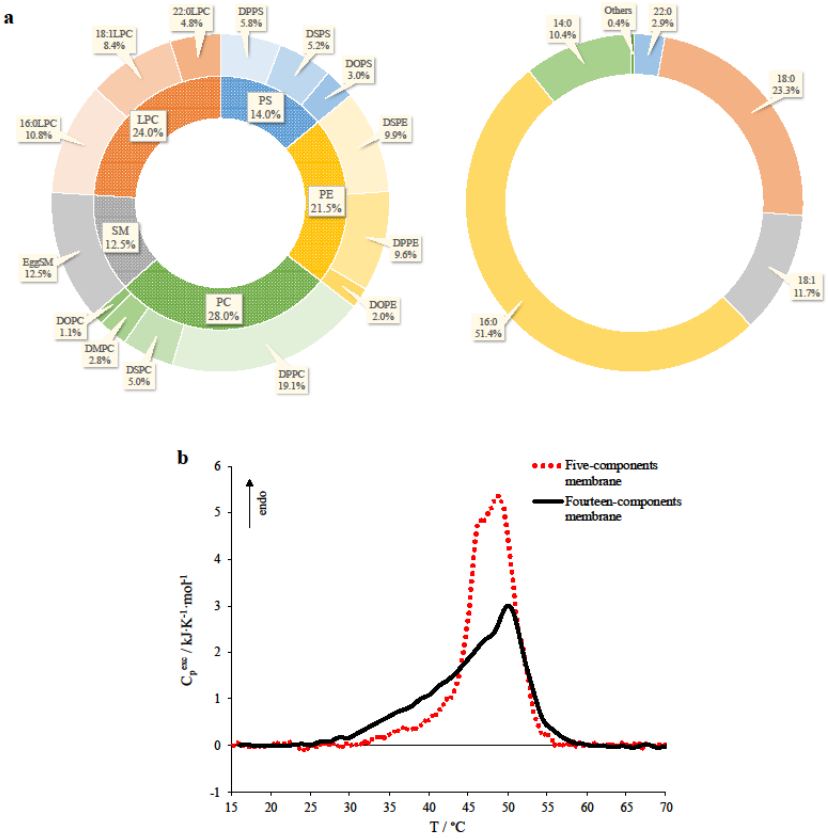

Fig.4

Micro-DSC thermograms obtained for a cholesterol-free fourteen-components membrane (black curve) and membranes with the addition of 10% and 20% of cholesterol (dashed green and dotted red curves, respectively).

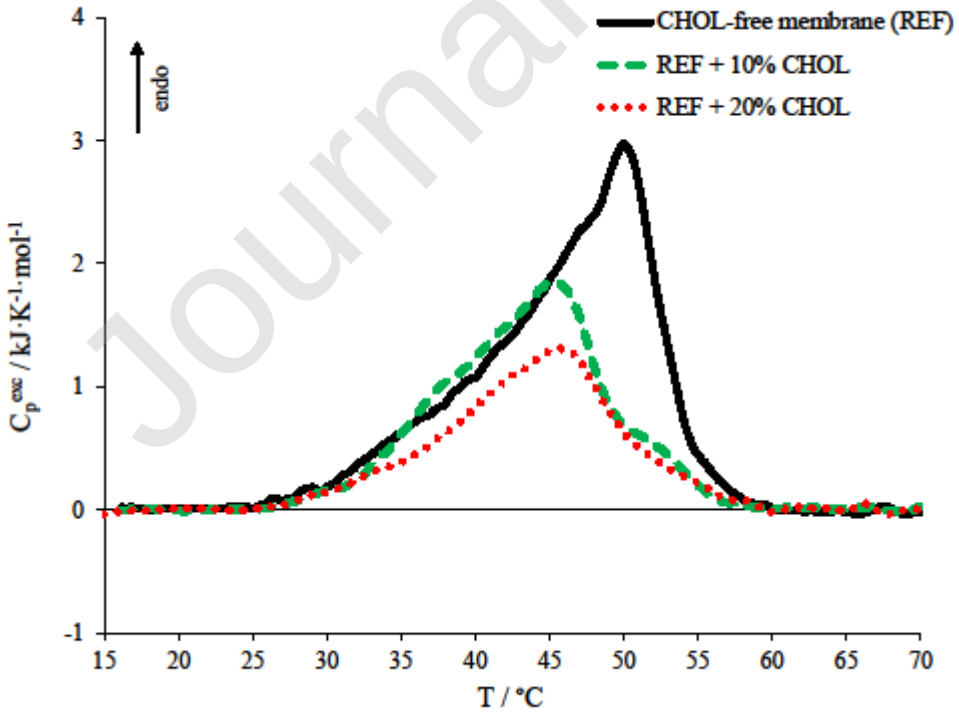

Fig.5

Micro-DSC profiles for the ISG-like vesicles (solid black curve) and vesicles with the addition of 20% FFAs. Thermograms are reported for membranes including stearic acid (dashed green curve) and oleic acid (dotted blue curve) in panel a, whereas elaidic acid (dashed red curve) is shown in panel b.

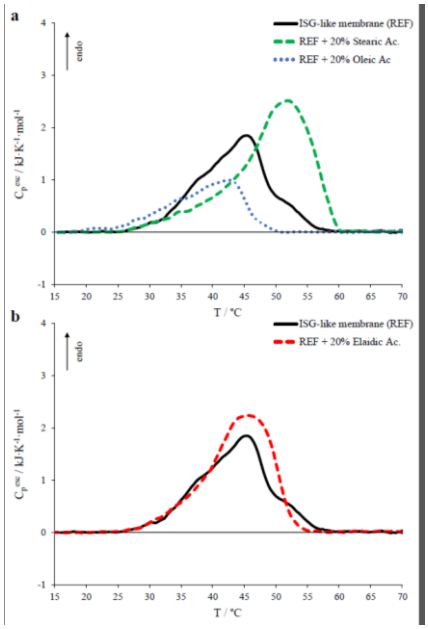

Table 1. Thermodynamic parameters evaluated from micro-DSC investigations for 1) binary systems and other representative mixtures and 2) ISG-like membranes and when possible compared with the arithmetical values calculated from single-component systems. The heating curves were used to obtain the main transition enthalpy ($\Delta H°$), the peak maximum temperature (T_{max}), the transition average temperature ($\bar{T}$) and the Average Cooperativity Index (ACI).

	Expected			Experimental			
	$\Delta H°$ kJ·mol^{-1}	$T_{expected}$ °C		$\Delta H°$ kJ·mol^{-1}	T_{max} °C	$\overline{T}$ °C	ACI °C
1. Binary systems and other representative mixtures							
DPPC:DPPS	38	48.3		37 ± 2	45.4 ± 0.2	46.5 ± 0.1	2.4 ± 0.1
DPPC:DPPE	36	53.1		36 ± 2	55.6 ± 0.3	53.1 ± 0.1	2.9 ± 0.1
DPPS:DPPE	38	59.8		37 ± 2	60.3 ± 0.2	59.5 ± 0.1	1.9 ± 0.2
Ternary membrane	36	52.3		36 ± 2	54.5 ± 0.2	52.4 ± 0.1	3.3 ± 0.1
Five-components membrane				42 ± 2	48.5 ± 0.5	47.2 ± 0.3	3.8 ± 0.2
2. ISG-like membranes							
Fourteen-components membrane				35 ± 2	50.4 ± 0.5	45.5 ± 0.3	6.3 ± 0.2
+10% CHOL				23 ± 2	44.8 ± 0.3	43.2 ± 0.3	5.7 ± 0.2
+20% CHOL				18 ± 2	46.4 ± 0.3	43.7 ± 0.3	6.0 ± 0.2
Fourteen-components membrane + 10% CHOL							
+20% Stearic Ac.				34 ± 2	52.1 ± 0.3	48.4 ± 0.3	6.6 ± 0.2
+20% Oleic Ac.				15 ± 2	42.6 ± 0.3	38.0 ± 0.3	5.8 ± 0.2
+20% Elaidic Ac.				29 ± 2	45.7 ± 0.3	43.5 ± 0.3	5.2 ± 0.2